Model-Based Estimation of Respiratory Parameters from Capnography, with Application to Diagnosing Obstructive Lung Disease

As Published: 10.1109/TBME.2017.2699972

Publisher: Institute of Electrical and Electronics Engineers (IEEE)

Persistent URL: https://hdl.handle.net/1721.1/134854

Version: Author's final manuscript: final author's manuscript post peer review, without publisher's formatting or copy editing

This article has been accepted for publication in a future issue of this journal, but has not been fully edited. Content may change prior to final publication. Citation information: DOI 10.1109/TBME.2017.2699972, IEEE Transactions on Biomedical Engineering

TBME-01625-2016

Model-Based Estimation of Respiratory Parameters from Capnography, with Application to Diagnosing Obstructive Lung Disease

Abubakar Abid, *Student Member*, *IEEE*, Rebecca J. Mieloszyk, *Student Member*, *IEEE*, George C. Verghese, *Fellow*, *IEEE*, Baruch S. Krauss, Thomas Heldt, *Senior Member*, *IEEE*

***Abstract*— *Objective:* We use a single-alveolar-compartment model to describe the partial pressure of carbon dioxide in exhaled breath, as recorded in time-based capnography. Respiratory parameters are estimated using this model and then related to the clinical status of patients with obstructive lung disease. *Methods*: Given appropriate assumptions, we derive an analytical solution of the model, describing the exhalation segment of the capnogram. This solution is parametrized by alveolar CO_2 concentration, dead-space fraction, and the time constant associated with exhalation. These quantities are estimated from individual capnogram data on a breath-by-breath basis. The model is applied to analyzing datasets from normal (n=22) and chronic obstructive pulmonary disease (COPD) (n=24) subjects, as well as from patients undergoing methacholine challenge testing for asthma (n=22). *Results*: A classifier based on linear discriminant analysis in logarithmic coordinates, using estimated dead-space fraction and exhalation time-constant as features, and trained on data from 5 normal and 5 COPD subjects, yielded an area under the receiver operating characteristic curve (AUC) of 0.99 in classifying the remaining 36 subjects as normal or COPD. Bootstrapping with 50 replicas yielded a 95% confidence interval of AUCs from 0.96 to 1.00. For patients undergoing methacholine challenge testing, qualitatively meaningful trends were observed in the parameter variations over the course of the test. *Significance*: A simple mechanistic model allows estimation of underlying respiratory parameters from the capnogram, and may be applied to diagnosis and monitoring of chronic and reversible obstructive lung disease.**

***Index Terms*—capnography, respiratory model, dead space, obstructive lung disease, COPD**

A. Abid and T. Heldt are with the Institute for Medical Engineering and Science, and the Department of Electrical Engineering and Computer Science, Massachusetts Institute of Technology, Cambridge, MA 02139 USA (e-mail: aabid93@mit.edu, thomas@mit.edu).

R. J. Mieloszyk was with the Research Laboratory of Electronics and the Department of Electrical Engineering and Computer Science, Massachusetts Institute of Technology. She is now with Philips Healthcare and the Department of Radiology, University of Washington, Seattle, WA 98195 USA (email: rjmielos@uw.edu).

G. C. Verghese is with the Research Laboratory of Electronics and the Department of Electrical Engineering and Computer Science, Massachusetts Institute of Technology, Cambridge, MA 02139 USA (e-mail: verghese@mit.edu).

B. S. Krauss is with the Division of Emergency Medicine, Boston Children's Hospital, Boston, MA 02115 USA, and the Department of Pediatrics, Harvard Medical School, Boston, MA 02115 USA (e-mail: baruch.krauss@childrens.harvard.edu).

I. Introduction

Capnography is the measurement of the partial pressure of carbon dioxide in exhaled breath ($peCO_2$), either as a function of time or of total exhaled volume. Time-based capnography is the predominant clinical modality [1], and is the focus of this paper, although the model presented in the paper can be adapted quite directly to volumetric capnography. The $peCO_2$ waveform, or capnogram, provides information about the ventilation and perfusion characteristics of the lungs [1, 2]. Unlike other pulmonary function tests, such as spirometry, capnography is effort-independent, as air exhaled by the subject during normal tidal breathing is drawn into the capnograph through a cannula placed in the nostrils.

Despite its convenience and ubiquitous presence in emergency departments, intensive care units, and ambulance services, the only quantitative uses of capnography in current clinical practice are to extract respiratory rate and end-tidal $peCO_2$ ($EtCO_2$); any further interpretation in the clinical setting is qualitative [1]. Our previous work has shown that the capnogram can be quantitatively analyzed, allowing machine learning algorithms to accurately discriminate between subjects with normal respiratory function and patients who have chronic obstructive pulmonary disease (COPD), and between COPD and congestive heart failure (CHF) patients (see Fig. 1), based on four capnogram features [3].

In this paper, we develop further tools to analyze the capnogram. We show that a simple mechanistic model for capnogram shape during the exhalation period of tidal

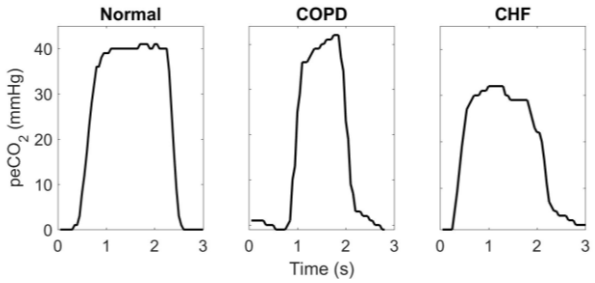

Figure 1: Representative normal, COPD, and CHF capnograms collected over one respiratory cycle [3]. The evident variations in morphology have motivated the use of the capnogram waveform for clinical assessment and diagnosis [1, 4].

This article has been accepted for publication in a future issue of this journal, but has not been fully edited. Content may change prior to final publication. Citation information: DOI 10.1109/TBME.2017.2699972, IEEE Transactions on Biomedical Engineering

breathing can be used to estimate underlying respiratory parameters. The estimates can be generated in real time and on a breath-by-breath basis, and can be used to classify subjects into different disease states.

Our mechanistic model is informed by compartmental models of the respiratory system that have been derived and studied over the last 60 years [5]. Many early models were developed with the goal of approximating the anatomy of the respiratory system, and thus included a large number of compartments, and representation of both diffusion and convection [6]. However, the number of parameters in such models greatly exceeds the limited number that can be estimated independently from a noninvasive measurement such as capnography. More recent studies of parameter estimation from capnography have used highly-simplified models of the respiratory system to express the capnogram in terms of a small number of parameters and associated differential equations [7, 8]. The choice of which respiratory parameters to include in such models determines the suitability of the model to a given application.

In this paper, we develop a simplified model with application to diagnosing obstructive lung disease. We design the model in terms of three parameters representing physiological quantities of clinical significance: dead-space fraction, respiratory time constant, and alveolar CO_2 concentration. By making particular assumptions about the pressure that drives airflow during exhalation, we derive a novel closed-form, double-exponential solution for the capnogram, described in terms of the three parameters. These parameters can then be estimated for a given subject by fitting the analytical solution to the measured capnogram.

We apply our model-based estimation framework to two tasks: (i) distinguishing between normal and COPD subjects on the basis of their capnograms; and (ii) tracking respiratory parameters across time in asthma patients who are undergoing methacholine challenge testing, a procedure that dynamically alters the patients' respiration. We addressed the former task in [3] by a very different (machine learning) approach; and preliminary explorations of the latter task using this model were presented in [9].

Section II of this paper derives our mechanistic model and its analytical solution. Section III discusses the data collection, preprocessing, and parameter estimation. In Section IV, we apply the model to discriminating between COPD patients and subjects with normal respiratory function. Section V applies the model to track respiratory parameters in asthma patients undergoing methacholine challenge. Section VI discusses the insights gained from these applications and the limitations of the model. We conclude in Section VII. Appendices A–D elaborate on aspects of the modeling and data analysis.

II. Mechanistic Model

In this section, we develop a mechanistic model for capnography, based on similar compartmental models of respiration previously introduced in the literature [7, 10]. As is generally the case with system identification, it is only possible to estimate a small number of parameters due to the limited richness of any real dataset [11, 12]. Thus, we aim to build a simplified model that aggregates respiratory features into a small number of independent variables and parameters relevant to diagnosing obstructive lung disease.

We begin modeling the capnogram by considering the total airflow through the respiratory tract. In spontaneous tidal breathing, the flow during exhalation is driven by an increased pleural pressure, caused by the contraction of the diaphragm and intercostal muscles [12]. This flow drives a second process, the mixing of CO_2-rich gas from the alveolar regions (defined as the parts of the respiratory system where gas exchange with the capillaries occurs) with the CO_2-poor gas in the anatomical dead space (defined as the upper respiratory tract, where gas exchange does not occur). After modeling these two processes, we solve the coupled differential equations to obtain a closed-form, analytical solution for the partial pressure of CO_2 in the dead space as a function of time, assuming a simple form for the change in pleural pressure. We take this partial pressure to be identical with $peCO_2$, the measurement recorded by the capnograph, see Fig. 2(a).

A. Airflow Process

Numerous mechanistic models have been proposed in the literature to describe airflow out of the lungs as a function of the driving pressure [13]. We use the simplest type of these models, which consists of a single alveolar compartment of variable volume, and a single compartment of constant volume to represent the anatomical dead space, as shown in Fig. 2(b).

The alveolar compartment is elastic, with a tissue compliance denoted by C_l. This compliance represents the linearized ratio of the change in volume of the alveolar compartment to the corresponding change in transmural pressure. The alveolar compartment is connected to the atmosphere through a pipe of air resistance R_l, representing the airway resistance of the dead space, specifically the conducting airways and oropharynx [13].

During spontaneous inhalation, the respiratory muscles contract, expanding the elastic compartment. During exhalation, the muscles relax, thereby allowing the lungs to deflate due to elastic recoil of the chest wall and lung tissue. This recoil increases the pleural pressure of the lungs by $P(t)$ above the pressure at the end of inhalation, as a function of time t after the start of exhalation. The differential equation for the resulting airflow, $\dot{V}(t)$, in this system is

$$\frac{d\dot{V}(t)}{dt} = -\frac{\dot{V}(t)}{R_l C_l} + \frac{\dot{P}(t)}{R_l} \tag{1}$$

This system can be represented by a circuit analog, as shown in Fig. 2(d). This circuit consists of a voltage source $P(t)$ driving a current $\dot{V}(t)$ through a series resistance R_l and capacitance C_l.

B. Gas-mixing Process

The time-based capnograph measures not the airflow but the partial pressure of CO_2 in air expelled from the respiratory system, so we proceed to model the mixing of gases in this volume during exhalation. Just prior to exhalation, the dead space is filled with atmospheric air containing negligible CO_2, (as in simpler models in the literature, the effects of

This article has been accepted for publication in a future issue of this journal, but has not been fully edited. Content may change prior to final publication. Citation information: DOI 10.1109/TBME.2017.2699972, IEEE Transactions on Biomedical Engineering

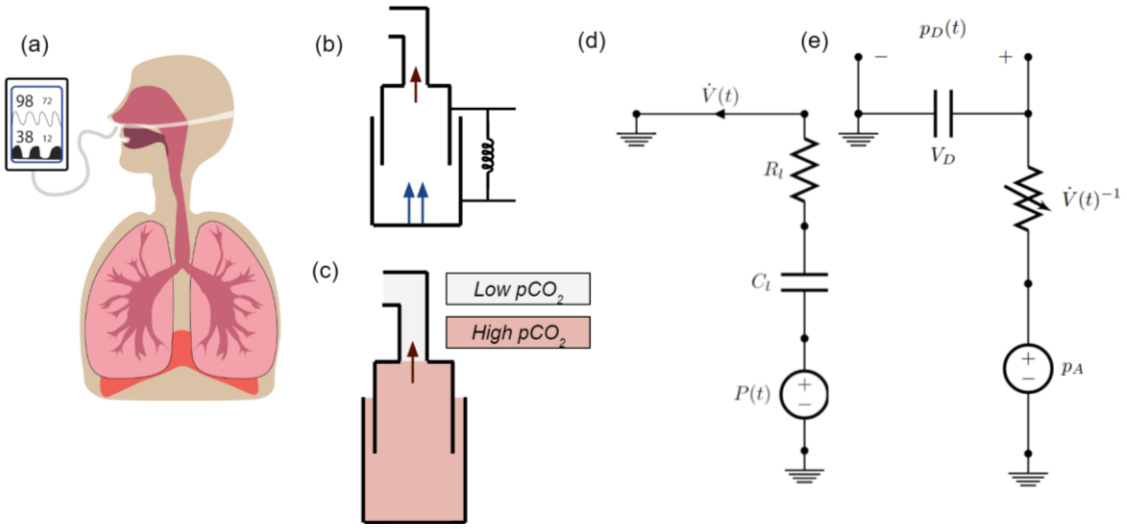

Figure 2: (a) The capnograph is connected to a subject through a nasal cannula, where it measures the partial pressure of carbon dioxide in air leaving the dead space. (b) The process of airflow can be abstractly represented by a spring-resistance model in which the alveolar compartment compresses during exhalation due to pressure exerted by the diaphragm and intercostal muscles (blue double arrow), which results in the airflow through a resistive pipe (red single arrow). (c) The process of mixing occurs as airflow mixes CO_2-rich air from the alveoli with CO_2-poor air in the dead space. (d) The process of airflow can be represented by the lumped-parameter circuit analog shown here, where voltage corresponds to fluid pressure, resistance to airway resistance, and capacitance to tissue compliance. (e) The process of gas mixing can similarly be represented in circuit form, but here voltage corresponds to the partial pressure of CO_2, capacitance corresponds to volume, and the variable resistance value is the inverse of volumetric airflow.

rebreathing CO_2 during inhalation are ignored [8]), while the gas in the alveolar region has substantial amounts of CO_2 due to gas exchange with the pulmonary capillaries. During the course of exhalation, the CO_2-rich gas from the alveoli mixes with the CO_2-poor gas in the dead space, as shown in Fig. 2(c). We assume this mixing is instantaneous because substantial mixing arises in the dead space through turbulence and airway branching [10, 13]. Small changes in alveolar CO_2 partial pressure during exhalation are ignored.

We now write a mass-transport equation for the partial pressure of CO_2 in the dead space, p_D. Suppose an infinitesimal amount of gas with CO_2 at partial pressure p_A enters the dead space and instantly mixes to create a homogenous mixture of gases in the dead space. Under the assumption that no mixing occurs in the alveolar compartment, then the mixing volume is effectively the dead space volume, V_D. To maintain a fixed volume and pressure of gas in the dead space, an infinitesimal amount of air is also expelled through the mouth and nose. The resulting differential equation for $p_D(t)$, the partial pressure of CO_2 in the dead space as a function of time t after the start of exhalation, is as follows:

$$\frac{dp_D(t)}{dt} = \frac{-p_D(t) + p_A}{V_D}\ \dot{V}(t) \qquad (2)$$

This subsystem can also be represented by a circuit analog, as shown in Fig. 2(e). In this circuit, unlike that of the airflow circuit, voltage corresponds to the partial pressure of CO_2. Thus, the constant voltage source p_A represents alveolar gas fixed at a constant partial pressure of CO_2. The charging of the capacitor with capacitance V_D represents the increase in CO_2 partial pressure in the dead space during exhalation. The rate of charging is modulated by a variable resistance equal to the inverse of the rate of airflow (which is modeled by the time-dependent current in the airflow circuit). The partial pressure of CO_2 in the dead space is $p_D(t)$, represented by the voltage on the capacitor as a function of time.

C. *Solution for a Step-Function Pressure Drive*

The coupled differential equations (1) and (2) can be solved for a general driving input, $P(t)$ (see Appendix A). For our present studies, we solve them for an explicit form of the input, namely when the driving pressure in (1) is a step function. This is motivated by the fact that measurements of pleural pressure in seated humans during tidal breathing show that $P(t)$ has a sharp increase at the beginning of exhalation and maintains a relatively steady value during the course of exhalation [14, 15].

Our assumption allows us to obtain a closed-form, analytical solution for the capnogram, expressed in terms of respiratory parameters relevant to diagnosing obstructive lung disease. This is in contrast to prior models of the capnogram, which include differential equations similar to (1) and (2), but assume certain functions for the airflow or include extra compartments and parameters, making a closed-form solution and parameter estimation more difficult [6–8].

To proceed, we write the change in pleural pressure, $P(t)$, during exhalation in terms of the unit step function $u(t)$ (which has the value 1 for $t \geq 0$ and the value 0 for $t < 0$):

$$P(t) = \Delta P \cdot u(t) \qquad (3)$$

where t is the time since the beginning of exhalation, and ΔP is the magnitude of the pressure step. Substituting (3) into (1)

This article has been accepted for publication in a future issue of this journal, but has not been fully edited. Content may change prior to final publication. Citation information: DOI 10.1109/TBME.2017.2699972, IEEE Transactions on Biomedical Engineering

and setting $\dot{V}(0) = 0$ at the start of exhalation, we find that the exhalation flow rate is given by

$$\dot{V}(t) = \frac{\Delta P}{R_l} e^{-\frac{t}{R_l C_l}} \quad (4)$$

Substituting (4) into (2) and assuming no rebreathing, so $p_D(0) = 0$, we find that

$$p_D(t) = p_A(1 - e^{-\alpha} e^{\alpha e^{-\frac{t}{\tau}}}) \quad (5)$$

In (5), $\tau = R_l C_l$ represents the pulmonary time constant [16]. The parameter α is defined by $\alpha = \frac{C_l \Delta P}{V_D} = \frac{V_T}{V_D}$ where the quantity $C_l \Delta P = V_T$ represents the tidal volume (assuming a linear pulmonary compliance [12]), so α is approximately the inverse of the pulmonary dead-space fraction [17]. Thus, an analytical expression for the time-based capnogram has been written entirely in terms of p_A, α and τ. We note that the latter two parameters represent quantities that are clinically relevant to the diagnosis of obstructive lung disease [16, 18].

Fig. 3 plots the double-exponential solution in (5) for different values of α and τ, including typical values in normal subjects (see Table I), while setting p_A to a value of 40 mmHg.

We note that an analogous procedure can be used to derive a simple analytical expression for volume-based capnography. This derivation is carried out in Appendix B.

III. Preprocessing and Parameter Estimation

In this section, we describe how the analytical solution in (5) is used to estimate respiratory parameters from two datasets. Each dataset consists of capnography measurements of variable length (between 2 and 20 minutes) taken from seated subjects wearing a nasal cannula connected to a portable capnograph (Capnostream 20, Covidien, Mansfield, Massachusetts). Measurements were recorded at a sampling frequency of 20 samples per second and an amplitude resolution of 1 mmHg. The subject populations varied between the two datasets and are described in Sections IV and V. For both datasets, study protocols were approved by the relevant Institutional Review Board, and informed consent was obtained from the subjects.

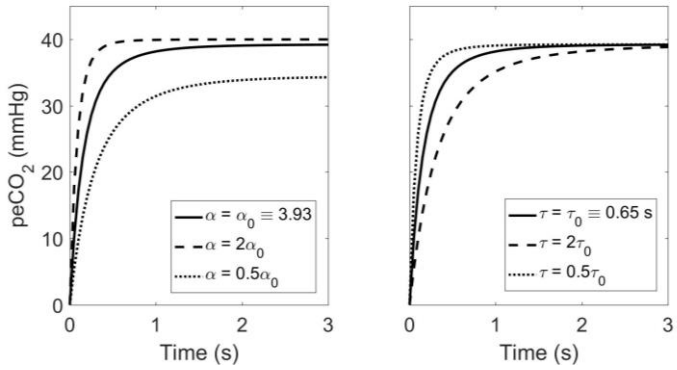

Figure 3: The analytical solution in (5) is plotted for various values for α (left) and τ (right). As can be observed from the plots, both α and τ affect the slope of the alveolar plateau, while α also affects the $EtCO_2$ level.

A. Preprocessing

Raw capnogram data were imported into MATLAB (MathWorks, Natick, Massachusetts) and preprocessed to extract individual exhalations. The preprocessing steps were performed to mitigate the effects of noise and artifacts, such as partial breaths and coughing.

The onset of an exhalation, for our purposes, was indicated by a reading of 1 mmHg or less immediately followed by a reading of 2 mmHg or more. (This ignores the interval during which any dead-space air that is unmixed with alveolar air is exhaled.) The end of an exhalation was indicated by a drop of 1 mmHg or more in measured partial pressure of CO_2 from one reading to the next. Exhalations that were less than 1.25 seconds long or more than 4 seconds long were excluded from consideration to minimize errors resulting from atypical exhalation waveforms. The resulting individual exhalation segments from a capnogram belonging to a normal subject are highlighted in Fig. 4 (top).

As can be seen in Fig. 4, the exhalatory segment of the capnogram was, in some cases, not captured in its entirety. This did not adversely affect parameter estimation, because the length of the analytical solution was set to match the length of the extracted segment before parameter estimation.

B. Parameter Estimation

The value of p_A in (5) was fixed for each patient to be the highest value of $peCO_2$ measured in their entire capnogram record. The parameter p_A was fixed because we found that the experimental data did not allow simultaneous identifiability of all three parameters in (5). This value was chosen because $peCO_2$ generally sets a lower bound on the value of p_A, and approaches p_A when the tidal volume is much larger than the volume of the dead space [19]. This choice was further supported by previous studies suggesting that $EtCO_2$ can be used as an estimate of p_A for the calculation of certain respiratory parameters [19].

With p_A chosen as above, the expression (5) was fitted to each valid exhalation segment independently – by searching over the space of τ and α to find the choice that minimized the mean-squared error between the analytical expression and the measured capnogram for that particular exhalation. This was done using MATLAB's gradient-descent-based, nonlinear, least-squares curve-fitting routine, `lsqcurvefit`. The parameters were each constrained to lie between 0.01 and 50 (the unit for τ being seconds); these bounds extend beyond normal physiological values [20–22]).

The breath-by-breath estimations of τ and α are shown for a capnogram chosen from a representative normal subject in Fig. 4. Exhalations that yielded poor fits (defined as cases where the sum of the squared of the residuals exceeded 4.8 $mmHg^2$, corresponding to the 75th percentile of normal exhalations) were rejected. A small number of exhalations produced atypically high values of α (greater than 9); those were similarly neglected. After removing exhalations that were too short or too long (in the pre-processing step) and those that produced a poor fit (in the parameter estimation step), 71% of normal exhalations remained and 51% of the COPD exhalations remained.

This article has been accepted for publication in a future issue of this journal, but has not been fully edited. Content may change prior to final publication. Citation information: DOI 10.1109/TBME.2017.2699972, IEEE Transactions on Biomedical Engineering

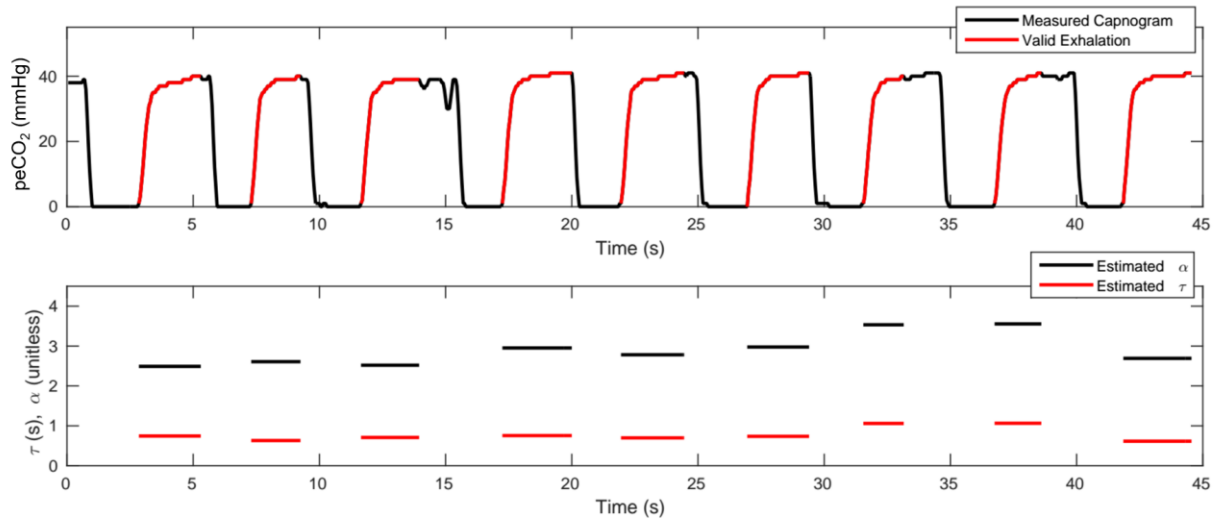

Figure 4: Exhalations were extracted from the raw capnogram record using an automated procedure that marked the onset of an exhalation as a rise in $peCO_2$ from 1 mmHg and the end of an exhalation by a decrease in $peCO_2$. The extracted exhalation segments are highlighted in red in the top plot, while the estimated parameters are shown in the graph below.

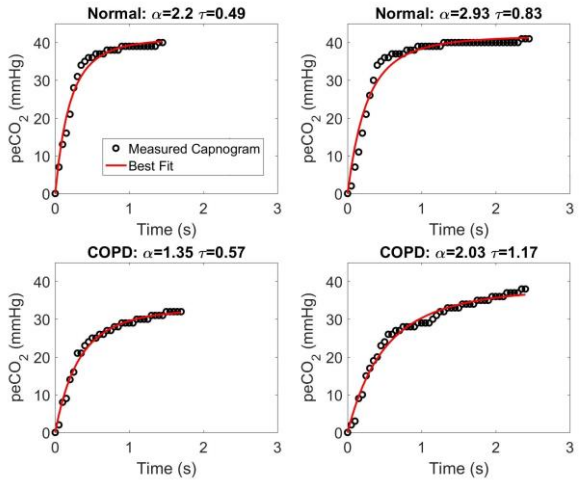

Figure 5: Sample exhalations from four individual capnograms, along with the corresponding curves produced by the model in (5) with the best-fit values of τ and α. The top two exhalations are from normal subjects, while the bottom two are from COPD patients.

Examples of the results typically produced by the fitting routine and parameter estimation are shown in Fig. 4 (bottom) and Fig. 5. These demonstrate that the model in (5) can represent the data well.

IV. Normal-COPD Classification

To determine whether differences in estimated parameter values can be used to reliably distinguish normal subjects from patients with COPD, the model was applied to a dataset consisting of 22 normal and 24 COPD subjects. The data were collected from subjects at Boston Children's Hospital, Boston, Massachusetts, and the Massachusetts Institute of Technology, Cambridge, Massachusetts (for normal subjects); and Einstein Medical Center, Philadelphia, Pennsylvania (for patients with COPD). Patient demographic information is summarized in Table I.

TABLE I
PATIENT DEMOGRAPHIC INFORMATION IN NORMAL-COPD STUDY

Class	Num. of Records (Test/Train)	Median Age (yrs.)	Age Range (yrs.)	% Female
Normal	24 (5/19)	25	21 – 59	41.7
COPD	22 (5/17)	61	43 – 82	63.6

Using the methods described in Section III, the parameters τ and α were extracted from all valid exhalations in each subject, and the mean values of τ and α were computed across all normal subjects and across all COPD subjects. Both parameters show general agreement with values reported in the literature for normal and COPD subjects (see Table II for the comparison).

The differences in the estimated parameter values between normal and COPD classes suggest that we could design a classifier to discriminate between COPD patients and normal subjects based on the estimated parameters. Fig. 6 shows the design of such a study, consisting of a training stage to calculate an optimal classifier, and a testing stage in which this classifier is used to label subjects as either COPD or normal.

TABLE II
REPORTED AND ESTIMATED PARAMETERS IN NORMAL, COPD SUBJECTS

Quantity	Mean Estimated Value [unit]	Reported Value [unit]	Reference
τ (normal)	0.84 [sec]	0.65[a] [sec]	[16]
τ (COPD)	1.09 [sec]	1.02[b] [sec]	[16]
α (normal)	2.97 [unitless]	3.33[c] [unitless]	[23]
α (COPD)	2.08 [unitless]	2.04[c] [unitless]	[22]

[a] Measured from patients who were mechanically ventilated for conditions other than COPD

[b] Measured from patients with "moderate COPD," the criteria for which are described in [17]

[c] The original works reported the mean dead-space fraction, and these are the reciprocal values

This article has been accepted for publication in a future issue of this journal, but has not been fully edited. Content may change prior to final publication. Citation information: DOI 10.1109/TBME.2017.2699972, IEEE Transactions on Biomedical Engineering

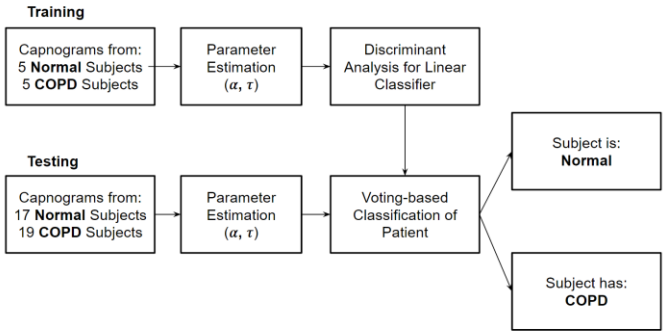

Figure 6: The design of the normal-COPD classification study: a subset of 5 normal subjects and 5 COPD patients were randomly selected for the training stage. A classifier was optimized for classification of individual exhalations as belonging to either COPD or normal subjects, based on the estimated values of τ and α). This optimal classifier was then used to diagnose the remaining 36 subjects in the testing stage. If the percentage of exhalations from the test subject that were classified as COPD exceeded a certain threshold, the subject was classified as COPD; otherwise, the subject was classified as normal.

A. *Training and Classifier Design*

The training set consisted of 5 COPD and 5 normal subjects randomly chosen from the study population. A total of 1,346 valid exhalations were extracted from these subjects. With p_A chosen for each record as described in Section III, the parameters τ and α were estimated for each of these 1,346 exhalations. Since the distribution of the parameters was found to be approximately log-normal (see Appendix C), a linear discriminant analysis [24] was performed in the $\ln(\tau)$–$\ln(\alpha)$ plane. The output of this analysis was a linear classifier: an exhalation whose parameters lay on one side of a separating line was classified as normal, while an exhalation on the other side was considered as belonging to a patient with COPD.

The discriminant analysis routine, `fitcdiscr`, in MATLAB was used to produce the linear classifier shown in Fig. 7 (indicated by the solid black line). The resulting classifier achieved an accuracy of 89.5% over all 1,346 exhalations in the training set.

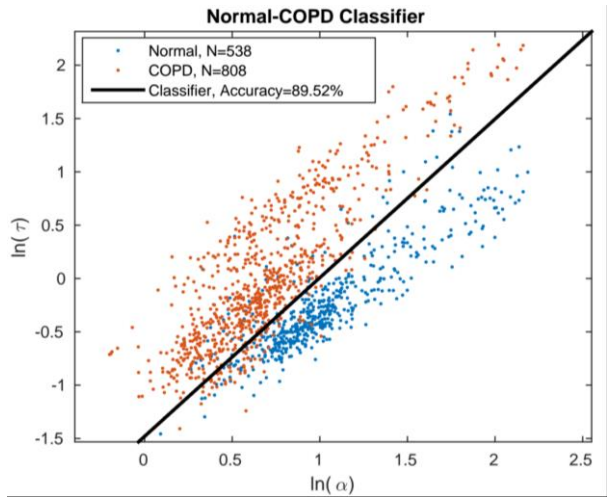

Figure 7: From the 1,346 exhalations in the training set, the linear classifier (solid black line) that optimally separated exhalations from COPD (parameters plotted in red) and normal (parameters plotted in blue) subjects was calculated. Some parameter ordered pairs lie outside the bounds of this axis and are omitted for ease of visualization.

B. *Testing and Classifier Performance*

This classifier was then tested on the remaining 36 subjects as follows. With p_A again chosen for each record as described in Section III, the parameters τ and α were estimated from every valid exhalation in each patient's record. Each exhalation was classified as either COPD or normal using the classifier developed in the training stage. Each exhalation thus acted as a voter that either cast a vote for normal or COPD. If the percentage of votes from a single patient for COPD exceeded a threshold (held constant across all subjects), the subject would be considered as having COPD; otherwise, the subject would be considered normal. Varying the threshold trades off specificity versus sensitivity, and yields a receiver operating characteristic (ROC) curve for the test.

The ROC curve, plotted in Fig. 8, shows that very high true-positive rates (TPRs) can be achieved by this classifier while keeping false-positive rates (FPRs) as low as 0.2. The test was bootstrapped by randomly selecting 50 patients with repetition from the test set, yielding a 95% confidence interval of area under ROC curve (AUC) values ranging from 0.96 to 1.00. Averaging the TPRs at each FPR level produces a (vertically averaged) ROC curve with an AUC of 0.99.

V. Methacholine Challenge

We describe here a further application of the model, to a dataset comprising patients with asthma – a reversible obstructive lung disease – undergoing a methacholine-challenge test. See Table III for the demographic information of the patients. The patients had all been referred to the pulmonary function lab at Beth Israel Deaconess Medical Center, Boston, Massachusetts, for methacholine challenge.

In this test, the pulmonary irritant methacholine is administered by inhalation in increasing doses. Subjects in whom this induces bronchospasm, as measured by a drop below 80% of baseline in the forced expiratory volume in 1 second (FEV1) assessed by spirometry, are considered to

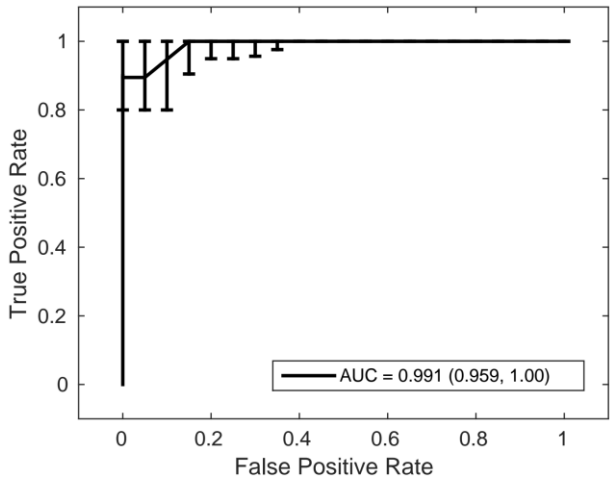

Figure 8: The ROC curve shown was produced by varying the percentage threshold of exhalations from a subject that needed to be classified as COPD for the subject to be classified as a COPD patient. Bootstrapping with 50 replicas yielded a 95% confidence interval of AUROC values, ranging from 0.96 to 1.00. The highest and lowest ROC curves in the 95% confidence interval are represented by the error bars, while the solid curve shows the ROC that is produced by averaging the values of the true positive rate at each false positive rate.

This article has been accepted for publication in a future issue of this journal, but has not been fully edited. Content may change prior to final publication. Citation information: DOI 10.1109/TBME.2017.2699972, IEEE Transactions on Biomedical Engineering

TABLE III
PATIENT DEMOGRAPHIC INFORMATION IN METHACHOLINE STUDY

Class	Num. Records	Median Age (yrs.)	Age Range (yrs.)	% Female
Methacholine (tested positive for asthma)	22	44	19 - 70	69.6

have tested positively for asthma. Our data set comprises only such positive subjects; those who did not respond significantly to the methacholine (negative subjects) were excluded from this study. All our (positive) subjects were treated with the bronchodilator albuterol at the conclusion of the methacholine challenge, to demonstrate reversal of the bronchospasm.

At each of the three stages – baseline (before methacholine was administered), post-methacholine (after the highest dosage of methacholine), and post-albuterol (after bronchodilator to reverse the effect of methacholine) – capnograms were recorded. The preprocessing and parameter estimation routine described in Section III were performed, to extract individual exhalations and their associated parameters. The value of p_A was taken as the maximum $EtCO_2$ value measured from the patient at any of the three stages. Thus, the value of p_A varied among patients, but not within a single patient. The parameters α and τ were estimated on an exhalation-by-exhalation basis for each stage for each patient. Finally, the variation of the median values of α and τ as the patients moved through the three stages was examined. The process is summarized in Fig. 9.

A. *Parameter Trends in Individual Patients*

The estimated parameters were observed to vary during the stages of the methacholine challenge. Fig. 10 shows the parameters from two patients. In both cases, the median value of α is observed to be lower in the methacholine stage, as compared to either the baseline or albuterol stages. Conversely, the median value of τ is observed to be highest in the methacholine stage.

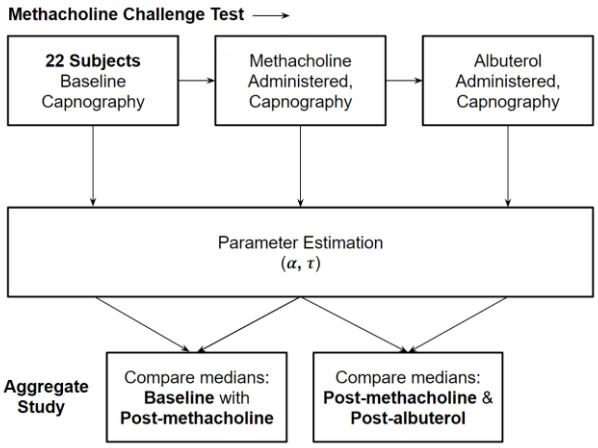

Figure 9: The dataset consists of 22 subjects who tested positive in the methacholine challenge. For these patients, capnograms were collected before methacholine was administered (at baseline), after the highest dose of methacholine was administered, and after albuterol was administered. The parameter estimation routine was performed on exhalations in each of these stages, and the median α and τ were calculated for each stage. For each patient, the shift in the median parameters was calculated to evaluate whether parameters shifted in consistent directions.

B. *Parameter Trends Across All Patients*

To observe whether these trends generalized to all patients, the median values for the estimates of τ and α were identified for each patient during each stage of the methacholine challenge. For each patient, the fractional shift of the median parameter values from the baseline to the post-methacholine challenge was noted, as was the fractional shift of the median values from post-methacholine to post-bronchodilator stage. These shifts, represented as 2D vectors in the τ-α plane, were aggregated across all 22 patients, and are plotted in Fig. 11.

The shift in parameters varied across patients, perhaps because patients began at different baselines, responded to methacholine to varying degrees, and did not always respond immediately. However, we found that the trends noted in the

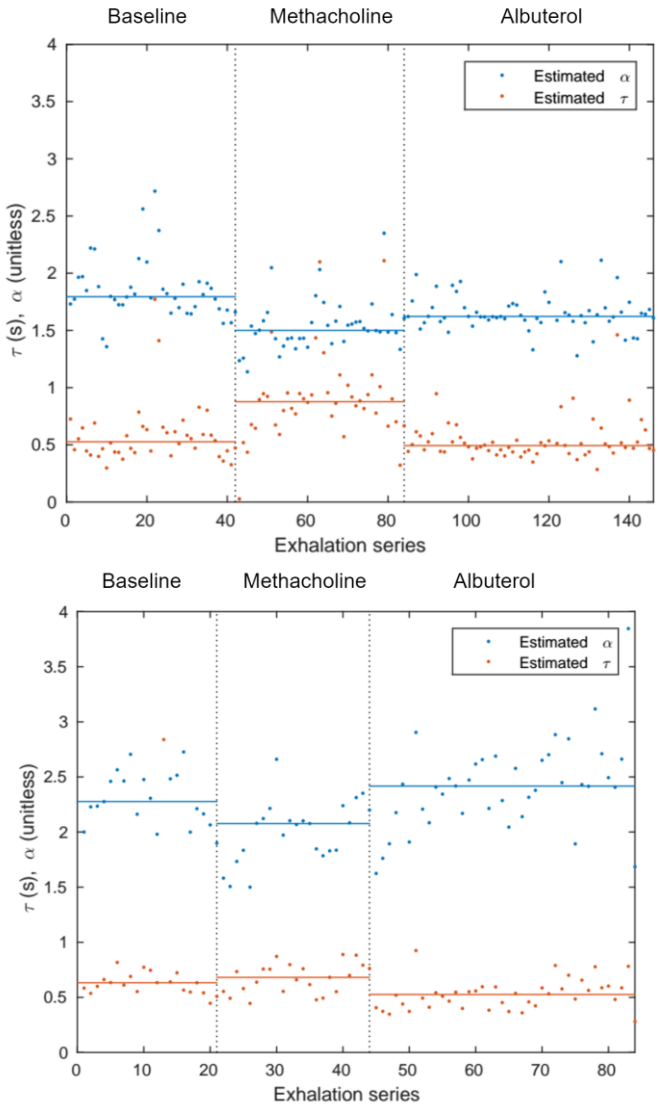

Figure 10: The results of parameter estimation from two patients are shown above. Each dot represents a parameter estimated from one exhalation, and the solid lines are the median values from all of the exhalations in each stage. In both patients, the median value of α decreased after the administration of methacholine and increased after the administration of albuterol. Conversely, the median value of τ increased after the administration of methacholine and decreased after the administration of albuterol.

This article has been accepted for publication in a future issue of this journal, but has not been fully edited. Content may change prior to final publication. Citation information: DOI 10.1109/TBME.2017.2699972, IEEE Transactions on Biomedical Engineering

previous subsection did generally hold in the larger patient sample. For example, in most patients (19 out of 22), the median value of α tended to be lower in the methacholine stage compared to baseline. In addition, in most patients (18 out of 22), α tended to be higher in the methacholine stage as compared to the albuterol stage. The opposite trend was generally observed with the parameter τ. In fact, in all but two cases, the administration of methacholine caused an increase in τ or a decrease in α or both, while the administration of albuterol conversely caused a decrease in τ or an increase in α or both.

Thus, as expected, the direction of parameter shifts due to methacholine was largely in the opposite direction of shifts due to albuterol. This is true not only on a population level but, as we show in Appendix D, also for each individual patient. Moreover, the directions of the shifts are consistent with experimentally-measured values in the literature. Higher lung resistance caused by narrowing of the respiratory tract (leading to increased τ) and higher physiological dead-space-volume-to-tidal-volume ratio (leading to decreased α) have been linked to methacholine administration, while the administration of bronchodilator is reported to have the opposite effect [20, 21].

VI. Discussion

We have derived an expression, (5), for $peCO_2$ as a function of time during tidal breathing, using a simple mechanistic model of the respiratory system. This expression provides good fits to measured $peCO_2$, as illustrated in Fig. 5, and allows estimation of physiologically meaningful respiratory parameters for each exhalation from capnograms of healthy subjects and patients with obstructive lung disease. Our results show that, despite the heterogeneity of the patient populations, the estimated parameters reflect patient physiological states, distinguishing between subjects in different clinical conditions, both chronically and acutely. Specifically, we have been able to discriminate with high accuracy between normal subjects and COPD patients (see Figs. 7 and 8) and to track induced bronchospasm and recovery for asthma patients undergoing methacholine challenge testing (see Figs. 10 and 11). More direct evaluation of the parameters estimated from our model could be made in future studies by comparing these estimates to more direct ones obtained, for example, by the forced oscillation technique [25] and volumetric capnography [26].

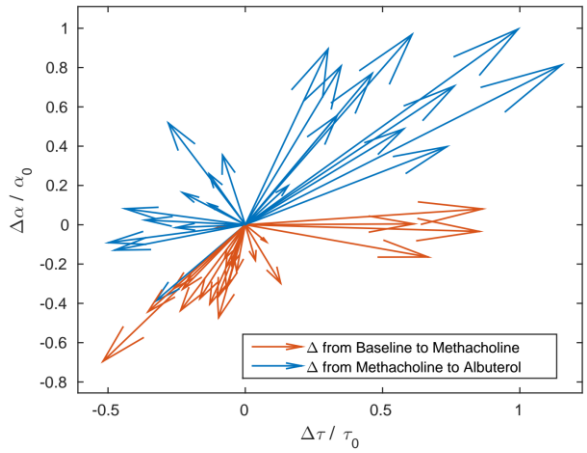

Figure 11: The fractional shift (change divided by original) between the stages in median values of τ and α were calculated for all 22 patients and are displayed as vectors in this plot. The shift after administration of methacholine tended to decrease α or increase τ, while the administration of bronchodilator had the opposite effect on parameter values.

The lumped-parameter model used in this paper makes certain simplifications to derive a closed-form solution for $peCO_2$. For instance, we model lung resistance and compliance as aggregate quantities, although they vary in different parts of the lungs [12]. Similarly, we compare α to the physiological dead-space fraction in the literature [18] even though it is more representative of the inverse of the anatomical dead-space fraction, which is less commonly cited in the literature. However, our model can be refined to better to address these limitations and capture complex lung dynamics in specific clinical settings. We can modify the model to include non-step pressure drives or non-linear compliances, for example, depending on the specific phenomena we are interested in modeling. A somewhat more detailed model representing the increased regional heterogeneity of lung resistance that is believed to occur in COPD patients [27] could be constructed by including a second dead space compartment. Similarly, our model is designed to be used with capnogram measurements during tidal breathing, but modifications (e.g. to the pressure sources) may allow it to be used with ventilated patients. Further extensions may include incorporating some representation of neural control of respiration [28, 29]. The trade-off in such refinements of the basic model is that more detailed models involve more parameters, which may not be reliably identifiable from clinical data of limited richness.

VII. Conclusion

We have proposed a mechanistic model that can estimate respiratory parameters from capnography. Previous studies have correlated morphological features of the capnogram to respiratory parameters and used these features for classification of obstructive lung disease [3, 5]. Our model of the respiratory system delivers a mechanistic, physiological explanation missing from prior studies and provides a means for clinicians to directly observe estimated respiratory parameters rather than relying on an automated classification scheme whose details may be hidden or difficult to understand.

Our results with healthy subjects and patients with obstructive lung disease suggest that a model-based approach to extracting respiratory parameters can be of practical diagnostic interest. Our work demonstrates that time-based capnography, which is noninvasive, effort-independent, and in ubiquitous use, has the potential to complement existing pulmonary function tests, such as spirometry, for screening and diagnosis of obstructive lung disease.

This article has been accepted for publication in a future issue of this journal, but has not been fully edited. Content may change prior to final publication. Citation information: DOI 10.1109/TBME.2017.2699972, IEEE Transactions on Biomedical Engineering

APPENDIX A: GENERAL SOLUTION FOR MECHANISTIC MODEL

In the paper, we present (5) as the solution of the mechanistic model, assuming that $P(t)$ takes the particular form given in (3). However, the mechanistic model can be solved analytically for a general $P(t)$. We derive that solution here.

The first-order, linear, time-invariant differential equation (1), with initial condition $\dot{V}(0-) = 0$ just prior to the start of exhalation, has the general solution

$$\dot{V}(t) = \frac{1}{R_l} e^{-\frac{t}{\tau}} \int_0^t e^{\frac{w}{\tau}} \dot{P}(w)\, dw \qquad (A2)$$

This will be time-varying in general, so the differential equation for the gas-mixing subsystem is a linear differential equation that includes a time varying-coefficient:

$$\frac{dp_D(t)}{dt} + p_D(t)\frac{\dot{V}(t)}{V_D} = p_A \frac{\dot{V}(t)}{V_D} \qquad (A3)$$

Since this time-varying system is also first-order, we can solve it explicitly to find a general, analytical solution for $p_D(t)$ in terms of $\dot{V}(t)$. Assuming no rebreathing for simplicity, we can take $p_D(0) = 0$, and then

$$p_D(t) = \frac{p_A \int_0^t e^{\int_0^w \frac{\dot{V}(x)}{V_D} dx} \dot{V}(w) dw}{V_D e^{\int_0^t \frac{\dot{V}(x)}{V_D} dx}} \qquad (A4)$$

APPENDIX B: ANALYTICAL EXPRESSION FOR MECHANISTIC MODEL OF THE VOLUMETRIC CAPNOGRAM

The volume-based capnogram plots the partial pressure of carbon dioxide as a function of total volume exhaled by the subject, instead of as a function of time. It is straightforward to derive an analytical expression for the volume-based capnogram using the mechanistic model proposed in Section II.

Assuming the same initial conditions and pressure drive, we solve (4) with the initial condition of $V(0-) = 0$ to get

$$V(t) = C_l \Delta P \left(1 - e^{-\frac{t}{R_l C_l}}\right) \qquad (B1)$$

Solving for t and substituting into (5), we find that

$$p_D(V) = p_A\left(1 - e^{-\frac{V}{V_D}}\right) \qquad (B2)$$

The result is a highly-simplified, first-order representation of the volumetric capnogram. We find that the solution no longer depends on the parameters τ and α, and is only parameterized by the dead space volume V_D and alveolar partial pressure p_A. This result would suggest that the dead space can be readily estimated from the volumetric capnogram, a conclusion supported by existing techniques to estimate dead space from volumetric capnography, such as Fowler's method [29].

APPENDIX C: LOG-NORMAL DISTRIBUTION OF RESPIRATORY PARAMETERS

The discriminant analysis presented in the paper above was performed in the $\ln(\tau)$–$\ln(\alpha)$ plane because the parameters are approximately log-normally distributed. The following figure demonstrates this qualitatively by plotting the natural logarithms of the parameters τ and α from the 5 normal and 5 COPD subjects in the training set in the study in Section IV, along with normal distributions with the same mean and standard deviation as the data.

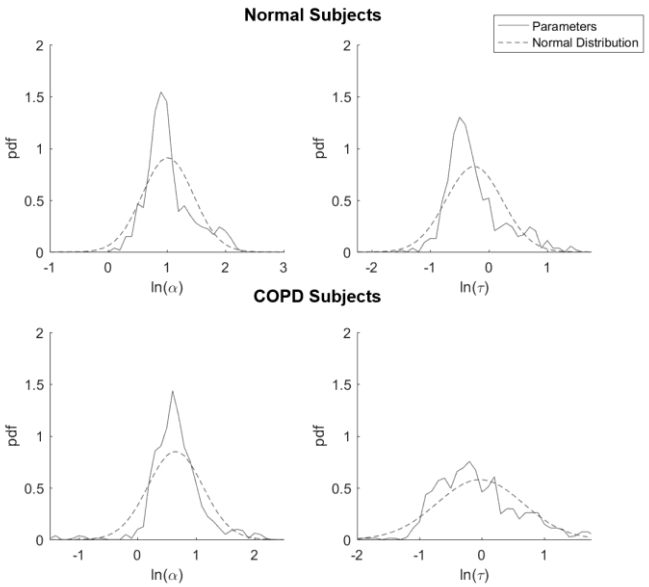

Figure C1: (Solid blue) the probability density functions describing the distribution of the natural logarithm of the respiratory parameters in normal and COPD subjects are shown, overlaid (red dashed) with the normal distribution that is generated with the same mean and standard deviation as the data.

While not shown here, the Kolmogorov-Smirnov test [30] was also performed and provided quantitative evidence that the logarithms of the parameters are more normally distributed than the original parameters themselves. This suggested that a linear discriminant analysis on the log-parameters would yield a better classifier than one performed on the original dataset.

APPENDIX D: PARAMETER SHIFTS AMONG INDIVIDUAL PATIENTS UNDERGOING METHACHOLINE CHALLENGE

In Fig. 11, we showed that the administration of methacholine, a pulmonary irritant, affects the estimated parameters in a qualitatively different way than the administration of albuterol, a bronchodilator. Across the 22 subjects in our study sample, the administration of methacholine generally increased α or decreased τ, while the administration of albuterol usually had the opposite effect.

Here, we consider the effect of methacholine and albuterol on individual patients. For each patient, we calculate the angle

between the vector that represents the fractional shift of τ and α due to the administration of methacholine (the red arrow in Fig. 11) and the vector that represents the fraction shift due to albuterol (the blue arrow in Fig. 11). The distribution of these angles for the 22 patients is shown in Fig. D1.

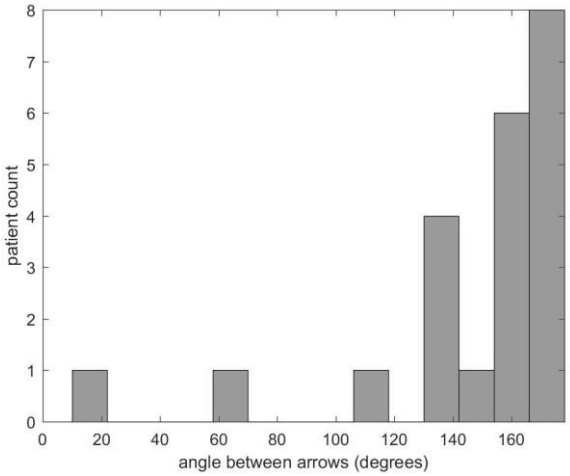

Figure D1: A histogram ($n = 14$ bins) of angles between the vector that represents the shift in parameters due to methacholine and the vector that represents the shift in parameters due to albuterol. 19 of the 22 angles are greater than 120 degrees.

The histogram shows that most of the angles are clustered near 180 degrees, suggesting that for most patients the direction of the parameter shifts due to methacholine was approximately opposite to the direction of the shifts due to albuterol.

ACKNOWLEDGMENT

We are grateful to Kenneth Deitch for collecting the COPD data used in our study from the Department of Emergency Medicine at Einstein Medical Center, Philadelphia. We thank Douglas Beach and Christy Smith from the Pulmonary Function Laboratory at the Beth Israel Deaconess Hospital for assistance with the methacholine study. We also thank Abdulrahman Alfozan and Abdullah Alsaeed for helpful comments on the design of the model, and Aneeqa Abid for help with the graphics included in this paper.

REFERENCES

[1] B. Krauss and D. R. Hess, "Capnography for procedural sedation and analgesia in the emergency department," *Annals of Emergency Medicine*, vol. 50, no. 2, pp. 172–81, 2007.

[2] R. Sikand *et al.*, "Effects of Va and Va/Q distribution and of time on the alveolar plateau," *Journal of Applied Physiology*, vol. 21, no. 4, pp. 1331–7, 1966.

[3] R. J. Mieloszyk *et al.*, "Automated quantitative analysis of capnogram shape for COPD–Normal and COPD–CHF classification," *IEEE Transactions on Biomedical Engineering*, vol. 61, no. 12, pp. 2882–90, 2014.

[4] B. You *et al.*, "Expiratory capnography in asthma," *Eur. Respir. J.*, vol. 7, 1994, pp. 318–323.

[5] A. B. Otis *et al.*, "Mechanical factors in distribution of pulmonary ventilation." *Journal of Applied Physiology*., vol. 8, no. 4, pp. 427-43, 1956.

[6] B. F. Peterman and A. Longtin, "Multicompartment model of lung dynamics." *Journal of Applied Physiology*, vol. 17, no. 6, pp. 580-9, 1984.

[7] J. O. D. Buijs *et al.*, "Bayesian tracking of a nonlinear model of the capnogram," *IEEE 2006 EMBS Annual International Conference*, pp. 2871–4, 2006.

[8] H. Benallal and T. Busso, "Analysis of end-tidal and arterial pCO_2 gradients using a breathing model," *European Journal of Applied Physiology*, vol. 83, no. 4-5, pp. 402–8, 2000.

[9] A. Abid *et al.*, "Model-based estimation of pulmonary compliance and resistance parameters from time-based capnography," *IEEE 2015 EMBS Annual International Conference*, pp. 1687–90, 2015.

[10] C. E. W. Hahn, "Gas exchange modelling: No more gills, please," *British Journal of Anaesthesia*, vol. 91, no. 1, pp. 2–15, 2003.

[11] T. Heldt *et al.*, "Mathematical modeling of physiological systems," in *Mathematical Modeling and Validation in Physiology: Applications to the Cardiovascular and Respiratory Systems*. J. J. Batzel, M. Bachar, and F. Kappel (eds). Berlin: Springer Verlag, 2013.

[12] J. Bates, *Lung Mechanics: An Inverse Modeling Approach*. New York: Cambridge University Press, pp. 9-42, 2009.

[13] J. B. West, *Respiratory Physiology*, Philadelphia, PA: Lippincott Williams & Wilkins, pp. 95–114, 2012.

[14] U. Lucangelo *et al.*, "Prognostic value of different dead space indices in mechanically ventilated patients with acute lung injury and ARDS," *Chest*, vol. 133, no. 1, pp. 62–71, 2008.

[15] R. Owens *et al.*, "Sitting and supine esophageal pressures in overweight and obese subjects," *Obesity*, vol. 20, no. 12, pp. 2354–60, 2012.

[16] D. Talmor and H. Fessler, "Are esophageal pressure measurements important in clinical decision-making in mechanically ventilated patients?" *Respiratory Care*, vol. 55, no. 2, pp. 162–71, 2010.

[17] M. Lourens *et al.*, "Expiratory time constants in mechanically ventilated patients with and without COPD," *Intensive Care Medicine*, vol. 26, no. 11, pp. 1612–8, 2000.

[18] T. J. Nuckton *et al.*, "Pulmonary dead-space fraction as a risk factor for death in the acute respiratory distress syndrome," *New England Journal of Medicine*, vol. 346, no. 17, pp. 1281–1286, 2002.

[19] G. Tusman *et al.*, "Validation of Bohr dead space measured by volumetric capnography," *Intensive Care Medicine*, vol. 37, no. 5, pp. 870–4, 2011.

[20] K. Olsson *et al.*, "Changes in airway dead space in response to methacholine provocation in normal subjects," *Clinical Physiology*, vol. 19, no. 5, pp. 426–32, 1999.

[21] J. Fish *et al.*, "Airway responses to methacholine in allergic and nonallergic subjects," *American Review of Respiratory Disease*, vol. 113, no. 5, pp. 579–86, 1976.

[22] R. Farah and N. Makhoul, "Can dead space fraction predict the length of mechanical ventilation in exacerbated COPD patients?" *International Journal of COPD*, vol. 4, pp. 437–41, 2009.
[23] R. D. Miller *et al.*, *Miller's Anesthesia*, 7th ed. Philadelphia: Elsevier, pp. 362, 2010
[24] A. J. Izenman, "Linear discriminant analysis," *Modern Multivariate Statistical Techniques*, Springer, pp. 237–80, 2013.
[25] E. Oostveen *et al.*, "The forced oscillation technique in clinical practice: Methodology, recommendations and future developments," *European Respiratory Journal*, vol. 22, no. 6, pp. 1026–41, Dec. 2003.
[26] R. Fletcher *et al.*, "The concept of deadspace with special reference to the single breath test for carbon dioxide," *British Journal of Anaesthesia*, vol. 53, no. 1, pp. 77–88, 1981.
[27] P. Burgel, "The role of small airways in obstructive airway diseases," *European Respiratory Review*, vol. 20, no. 119, pp. 23–33, 2011.
[28] E. M. Wagner and D. B. Jacoby, "Methacholine causes reflex bronchoconstriction," *Journal of Applied Physiology*, vol. 86, no. 1, pp. 294-7, 1999.
[29] A. J. Berger *et al.*, "Regulation of respiration," *New England Journal of Medicine*, vol. 297, no. 4, pp. 194–201, Jul. 1977.
[30] M. H. DeGroot and M. Schervish, "Kolmogorov-Smirnov Tests," in *Probability and Statistics*, 4th ed. Boston, MA: Addison Wesley, ch. 10, sec. 6, pp. 657–65, 2012.